3E Analysis of a Trigeneration System for Heat, Water, and Power Production

Norouzi, Nima
Department of Energy Engineering and Physics, Amirkabir University of Technology (Tehran Polytechnic), Tehran, I.R. IRAN

Bozorgian, Alireza*+
Department of Chemical Engineering, Mahshahr Branch, Islamic Azad University, Mahshahr, I.R. IRAN

ABSTRACT: *With climatic conditions and close to flooding areas for the system under construction, an energy production system using two types of renewable energy, estuary, and wind, has favorable wind speed conditions. The Steam cycle is designed with a parabolic-linear collector to maximize the use of the heat generated by the system, which is then transferred by an evaporator and a steam turbine to produce energy. The evaporator must generate a single-effect absorption refrigeration system to generate a cooling load. Its main components are a steam-Rankine cycle, organic Rankine cycle, thermoelectric, absorption refrigeration, reverse osmosis, and a parabolic-linear manifold. The system was modeled using EES software to obtain thermodynamic results. Based on the results, solar systems with a central receiver have the highest energy losses. The exergy analysis revealed that the solar system has 60%, and the wind turbines have 17% of the system's exergy losses*.

KEYWORDS: *Solar system; Steam cycle; Absorption refrigeration cycle; Reverse osmosis desalination plant; Wind turbine.*

INTRODUCTION

Due to the industrialization of most cities, energy demand grew significantly. The continuous increase in energy demand has led to the widespread use of carbon-containing fossil fuels, which has caused significant damage to the environment and human health. In recent years, many efforts and programs have been made to reduce the use of fossil fuels. Renewable energy sources such as solar and wind have been introduced as reliable sources for clean energy production. Solar power plant technology using parabolic-linear concentrators is the most significant method among thermal-electric methods for renewable energy production.

In 2020, *Kumar Gupta et al*. [1] proposed a proposed system consisting of an organic Rankin cycle with a triple-pressure level absorption system and a parabolic-linear solar collector system. This system generates electricity and refrigeration simultaneously at two different temperatures. This study investigated the effect of different inlet parameters such as solar radiation, turbine inlet pressure, turbine outlet pressure, and evaporator temperature on the schematic subsystems. In 2020, *Dubkram et al*. [2] thermodynamically analyzed a multiple power generation system by thermal energy from a solar system of a parabolic-linear solar collector. The results

* *To whom correspondence should be addressed.*
+E-mail address: alireza.bozorgian@iau.ac.ir
1021-9986/2022/12/1343-1355 13/$/6.03

showed that increasing the turbine inlet temperature increased efficiency and decreased overall energy losses. The results also showed that the two main sources of exergy losses are the solar system and the desalination unit.

In 2020, *Alirehmi et al*. [3] proposed a multiple-generation system based on geothermal energy and a parabolic-linear solar collector system for simultaneous electricity generation, cooling load, freshwater, hydrogen, and heat. To optimize the objectives of this research, EES and MATLAB software were interconnected using the Dynamic Exchange Data method. Finally, the system's efficiency and total unit cost were 29.95% and 129.7 $/GJ, respectively.

In 2020, *Al-Otaibi et al*. [4] investigated the performance of a conventional steam power plant with a regenerative system equipped with a parabolic-linear solar collector system. The system analysis results showed that removing the LP turbine increases the performance of the steam power plant up to 9.8 MW / h. The optimal area for the solar system in these conditions was estimated at 25,850 square meters.

In 2019, *Ahyaee et al*. [5] conducted thermodynamic analysis, energy and exergy, and economic analysis using a linear parabolic solar collector. The optimization results showed that the exergy efficiency, energy efficiency, and costs are 29.29%, 35.55%, and $ 0.0142/kWh, respectively. In 2019, *Toghyani et al*. [6] used a nanofluid fluid in a parabolic-linear solar collector to cool the solar system and produce hydrogen. The results show that hydrogen production increases under higher solar intensities because the Rankin cycle transfers more energy to the PEM.

Al-Zahrani and *Dincer* [7], 2018, studied the energy and exergy of parabolic-linear solar collectors as part of a solar power plant under different design and performance conditions. Finally, the energy and exergy efficiency rates of 35.66% and 38.55% were reported, respectively. In 2019, Yilmaz [8] reviewed the comprehensive thermodynamic performance and economic evaluation of a combined ocean thermal energy system and a wind farm. The results show that the hybrid system's overall energy and exergy efficiencies are 12.27% and 34.34%, respectively. The cost of the proposed system was reported to be $ 3.03 per hour. *Isaac & Dincer* [9] In 2020, a new idea for hydrogen production using wind energy and methanol application. The proposed system used industrial carbon emissions to produce methanol. EES and Aspen Plus software were used to model and analyze the system. *Bamisile et al* (2020) [10] modeled a power generation system using wind, solar, and biogas energy and analyzed the system's energy and exergy. The results showed that the system's overall energy efficiency varies from 64.91% to 71.06%, while the exergoeconomic efficiency increases from 31.80% to 53.81%. In 2018, *Kianfard et al*. [11] investigated a renewable system to produce fresh water and hydrogen-based thermal energy. The results showed that the investment costs per unit of reverse osmosis desalination plant were obtained by economic analysis with 56%. The cost of producing freshwater was estimated at 32.73 cents per cubic meter.

Ali Rahmi and *Asareh* [12] In 2020, analyzed the energy, exergy, and economy and multi-objective optimization of multiple energy systems, including hydrogen production, freshwater, cooling, heating, hot water, and electricity in Dezful city. The two objective functions of this study were exergy and total cost, which were optimized by a genetic algorithm. Finally, the best value for exergy efficiency was 31.66%, and the total unit rate was 21.9 $/GJ. In 2020, *Mohammadi et al*. [13] designed a combined cycle gas turbine to generate electricity, freshwater, and cooling. The results showed that reverse osmosis is more economical than a combined MED-RO system. System costs for electricity, water, and cooling were also reported at $ 0.0648 per kilowatt-hour, $ 0.7219 per cubic meter, and $ 0.0402 per hour, respectively.

A study by *Haghanimanesh et al*. [14] presents an analysis of a combined heating, cooling and power cycle that recovers the thermal energy of waste steel slag. The cycle utilizes the biogas produced from anaerobic digestion process of wastewater and sewage of residential areas. A thermodynamic model used for the trigeneration cycle and the performance of the cycle investigated from exergy and exergy-economic aspects. The power production capacity of the cycle, the cooling capacity and hot water production rate achieved 700 kW, 40 tons of refrigeration and 29400 kg/h, respectively. Also, the results of exergy-economic analysis indicate that the costs of power exergy, cooling and heating produced by the combined cycle are 30.14 $/h, 28.73 $/h and 29.25 $/h, respectively. Among six working fluids that examined for the organic Rankine cycle, R123 had the highest efficiencies (16% to 28%) in the turbine inlet temperature range of 200 °C to 420 °C and the highest output power was about 50 kW. Moreover, the highest growth rate of exergy efficiency and power generation in this temperature range observed when HFE7000 used as the working fluid.

In research by *Fakhari et al*. [15], a tri-generation combined cycle is presented. This proposed system is equipped with a triple-pressure heat recovery steam generator with a novel configuration of heat exchangers to exploit the maximum possible waste heat. The gas turbine cycle also utilizes Parabolic Trough Solar Collectors to reduce fuel consumption and CO_2 emission. The low-pressure steam of the heat recovery steam generator is used as the motive steam of a multi-effect desalination unit for freshwater production, and the heat rejection of the steam cycle is utilized in a double-effect absorption chiller to generate a cooling load. According to these modifications, the HRSG exhaust has considerable energy after the low-pressure steam of the heat recovery steam generator; hence, an organic Rankine cycle with a zeotropic mixture as working fluid is used to recover the energy. The proposed model is implemented in MATLAB software, and the energy, exergy, economic and environmental analyses are conducted on the model. Five single- and multi-criteria optimizations are conducted to determine the proposed system's optimum operating condition from different aspects. The results are presented as 2D and 3D Pareto Frontiers. A comparative study on scatters of distribution is presented as a novel approach to investigate each optimization objective's effect on decision variables through single- or multi-objective optimization. Referring to analyses utilizing the solar collectors mitigate the fuel consumption from 6.31 kg/s to 6.01 kg/s and results in a decrease of 0.81 kg/s CO_2 production. Besides, the waste heat recovery in the heat recovery steam generator attained a 20.17% exergy efficiency increase as well as 181.82 m3/h freshwater production and 5.98 MW cooling load as the secondary outputs and rose the power production from 74.87 MW to 140.92 MW. The best point on the 3D Pareto Frontier of the tri-objective optimization obtained the exergy efficiency of 45.86%, the total cost rate of 1.161$/s, and the CO_2 emission of 17.05 kg/s.

In a study by *Musharavati et al*. [16], a poly-generation system including a Kalina cycle, a reverse osmosis unit, a PEM electrolyzer and a thermoelectric module that can generate power, fresh water, hot water, and hydrogen are examined. A thermodynamic simulation code in Engineering Equation Solver (EES) is prepared to predict the behavior of system. Using the exergy analysis different location of system with high irreversibility are determined. As the results show in the base case, the geothermal cycle condenser with 89.29 kW, reverse osmosis (RO) unit with 68.97 kW, heat exchanger 2 with 37.68 kW, and steam turbine with 22.52 kW have the highest exergy destruction rate respectively. The parametric analysis for identifying the influence of five decision variables namely steam turbine inlet pressure (P2), steam turbine back pressure (P4), vapor generator outlet pressure (P10), Kalina turbine backpressure (P13), and temperature difference of the heat exchanger (TD) is conducted. Additionally, four major outputs consisting of exergy destruction rate (kW), exergy destruction cost rate ($/h), and electricity cost rate ($/h) are determined for implementing multi-criteria optimization. A tri-objective optimization to find the optimum states of the suggested system is conducted. With employing a selection method, the system arrangement with 328.2 kW of exergy destruction rate, 18.4 $/h of exergy destruction cost rate, and 12.83 $/h of electricity cost rate with determined value of decision variables is selected as final optimum state.

Considering the thermal processes with the help of smart heat recovery, A study by *Cao et al*. [17] proposes a novel auxiliary trigeneration system for a ship based on the waste heat of its engine to produce electricity, cooling, and freshwater. The system consists of a regenerative organic Rankine cycle (RORC) with R600 working fluid, a lithium-bromide/water single-effect absorption chiller, and a Humidification DeHumidification (HDH) desalination unit. A multi-heat recovery technique is implemented in the design framework, having a well-organized waste-to-energy system. Technical 3E (energy, exergy, and exergoeconomic) analysis together with a multi-criteria optimization using a genetic algorithm is conducted. Furthermore, a parametric study is employed regarding the impact of changing design parameters, namely, pinch point temperature difference of the High Recovery Vapor Generator (HRVG), turbine inlet pressure, and top temperature of the HDH on the thermodynamic and exergoeconomic criteria. The results indicated the high sensitivity of the outputs from varying the turbine inlet pressure. Besides, the optimum net output power, cooling, and generated freshwater are calculated to be 783.9 kW, 959.8 kW, and 98.1 m^3/day, respectively. Also, the optimum energy and exergy efficiencies and total cost per unit exergy are computed to be 58.4%, 43.0%, and 0.1494 $/kWh, respectively.

A study by *Zhou et al*. [18] authenticates that the waste heat of a geothermal steam flash cycle is recuperated efficiently via embedding an organic flash cycle and an

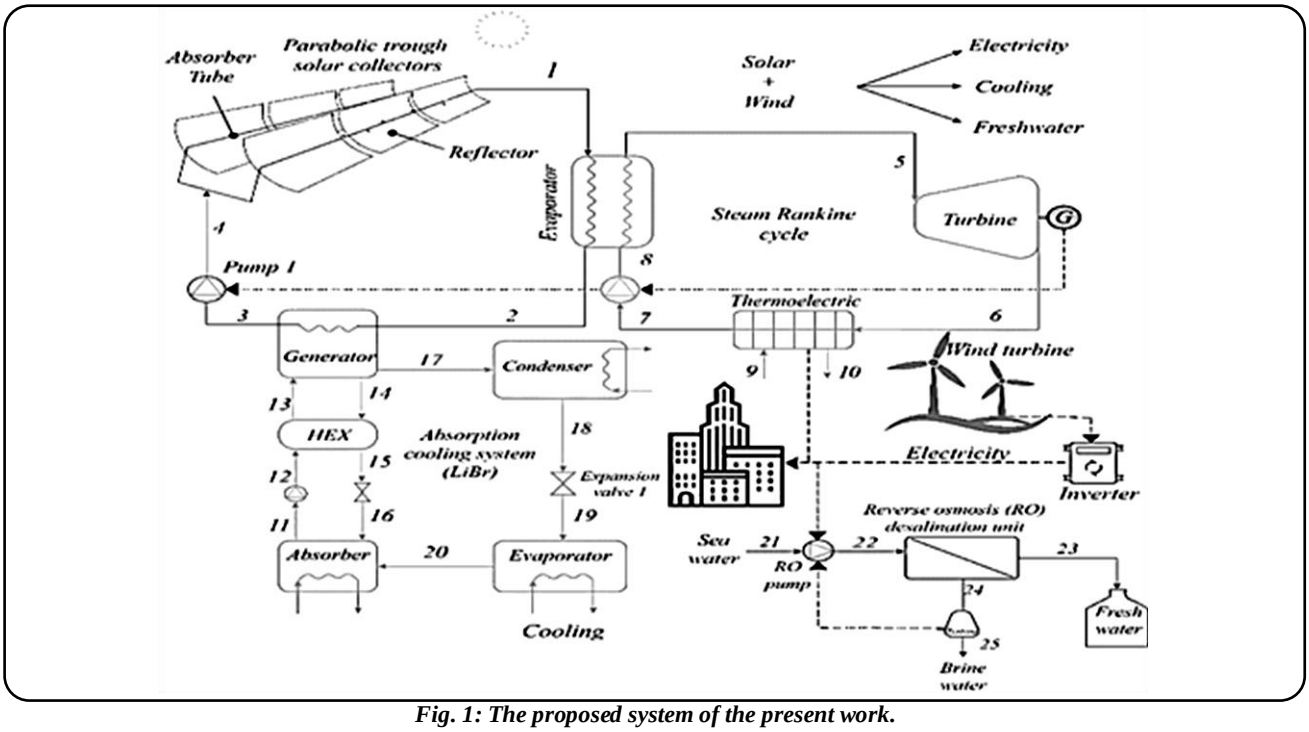

Fig. 1: The proposed system of the present work.

$LiCl–H_2O$ absorption refrigeration system in the high-temperature flow path and placing a hot water production unit in the low-temperature flow path. Consequently, the waste heat of both high and low-temperature flows of the steam flash cycle is recovered. There is still heat loss in the organic flash cycle that has the potential to be recovered. In this respect, an expander and a thermoelectric generator are respectively employed instead of the throttling valve and condenser of the organic flash cycle to convert the waste energy of the organic flash cycle into power. The overall power generated in the organic flash cycle is transmitted to an electrolysis unit to produce hydrogen. The multi-objective optimization of the designed system indicates an exergy efficiency of 30.89%, which is 15.74% points higher than the case for the sole generation of electricity by the steam flash cycle. At the optimal point, the rates of output work, heating, cooling, and hydrogen are equal to 757.1 kW, 8567 kW, 3017 kW, and 1.627 kg/h, respectively. The comparison between the performance of the system and three similar geothermal-based systems for polygeneration purposes reveals that in addition to the highest exergy efficiency, the proposed system is superior in terms of the unit cost of polygeneration, with a value of 5.98 $/GJ.

This study investigated a renewable system using solar and wind energy. In this system, a parabolic-linear collector was used as a source of thermal energy supply, and a wind turbine was used as a direct source of electricity, one of the innovations of the present work of combining solar and wind systems to increase efficiency and system production. Due to the unavailability of solar energy at all hours of the day, wind energy to help supply the energy required by the system was considered. Another innovation of this system is parabolic solar collectors because, according to previous studies, more flat-panel solar collectors have been used, and other collectors such as parabolic collectors have received less attention. Another innovation of this research is thermoelectric instead of the condenser in the Rankin organic cycle, which helps increase the system's production capacity and perform a condenser's function. The system consisted of a flat panel solar collector, wind turbine, Rankine cycle, and thermoelectric use. EES software is used as an engineering tool to model the system and obtain thermodynamic results.

CASE STUDY

Figure 1 shows a schematic of the multiple energy generation systems under consideration. To use the heat from the solar system with a parabolic-linear collector, a steam cycle is designed in which heat is transferred through an evaporator and generates electrical energy through a steam turbine. The heat remaining after the steam

Table 1. Input parameters.

Parameter	unit	Value
Tsun	[k]	5800
T_1	[c]	320
G_b	[W/m^2]	900
U_l	[w/m^{2}C]	3.82
P_5	[kpa]	1500
P_7	[kpa]	100
Ηpump	-	0.9
Ηturbine	-	0.85
ppeva	[c]	5
T20	[c]	6
T14	[c]	90
T13	[c]	65
T17	[c]	85
Ave_Wind_speed	[m/s]	5.5
Windefficiency	-	0.9
Powerecoefficiency	-	0.59
Diameter	[m]	34

cycle evaporator generates an absorption refrigeration system to generate a cooling load. In this system, reverse osmosis is used to produce fresh water. A steam turbine supplies the electricity required for reverse osmosis desalination water.

The main components of the solar energy system are linear-parabolic collector, steam cycle, absorption refrigeration system, wind turbine, reverse osmosis desalination plant, and a thermoelectric generator. A heated oil system (state 1) first enters the evaporator and then transfers its heat to the steam cycle. Then the remaining heat from the gas turbine enters a thermoelectric, and the system converts the received heat into electrical energy. A freshwater supply is provided that receives its required electricity from the gas turbine. The remaining heat from the steam cycle evaporator enters the absorption refrigeration cycle generator and provides the heat required to generate the cooling load.

The inputs required for system modeling are listed in Table 1.

METHODOLOGY

Using the following equation, the amount of useful energy produced in PTCs is obtained:

$$\dot{Q}_u = n_{cp} n_{cs} F_R (S A_a - A_r U_L (T_{ri} - T_0) \quad (1)$$

The value of *S* is calculated from the following equation:

$$S = G_b \eta_r \quad (2)$$

$$\eta_r = \gamma \tau_C \tau_P \alpha \quad (3)$$

The following equations specify the parameters F1 and FR:

$$F_R = \frac{m_c C_{p,c}}{A_r U_L}\left(1 - \exp\left(-\frac{A_r U_L F_1}{m_c C_{p,c}}\right)\right) \quad (4)$$

$$F_1 = \frac{\frac{1}{U_L}}{\frac{1}{U_L} + \frac{D_{o,r}}{h_{fi}} + \left(\frac{D_{o,r}}{2k}\ln\left(\frac{D_{o,r}}{D_{i,r}}\right)\right)} \quad (5)$$

Using the following relation, the area of parabolic-linear collectors is determined:

$$A_a = (w - D_{o,r})L \quad (6)$$

The power generated by the wind turbine, taking into account the values of the average annual wind speed, is written as follows:

$$w_{wind\_turbine} = \frac{1}{2\eta_{wt}\rho_{air}A_{wt}C_{p,wt}v^3} \quad (7)$$

Where $w_{wind,\ turbine}$ is the wind turbine's output of the wind turbine, and ηwt is the efficiency, ρ_{air} is the air density, and *V* is the wind speed. The total net output of the system is calculated from the following equation:

$$w_{net} = W_{turbine} + W_{wind,turbine} + W_{TEG} - W_{pump,2} - W_{pump,1} \quad (8)$$

The return on investment can be defined as follows [14]:

$$CFR = \frac{ix(1+i)^n}{(1+i)^n - 1} \quad (9)$$

Here, *i* and n show the profit and operating period of the plant (year), which are equal to 0.1 and 20, respectively.

Since each device of a hybrid system is expected to operate in a specific time pattern, the cost rate of each device is a good measure of the cost rate denoted by Z.

The cost rate of each device is calculated from the following equation [14]:

$$Z = \frac{Z_{total} CRF \Phi}{T} \quad (10)$$

Indicates the cost of cycle components, Z_{total} is the total cost. In addition, *T* is the annual operating hours (number of working hours), $\emptyset$ is the maintenance factor.

The total cost of the system is calculated from the following equation:

$$Z_{total} = Z_{turbine} + Z_{TEG} + Z_{pump,2} + Z_{pump,1} + Z_{evap,1} + Z_{solar} + Z_{RO} + Z_{chiller} + Z_{wind,turbine} \quad (11)$$

Reverse osmosis is a desalination technology based on the use of membranes. The desalination process also allows the filtration of the smallest components of the solution. Therefore, the reverse osmosis process can be used to purify the water. According to the operation of reverse osmosis desalination plants, the amount of water flow rate is calculated using the freshwater flow rate at state 38 and the RR reversibility coefficient from the following equation [15-17]:

$$m_{43} = \frac{m_{45}}{RR} \quad (12)$$

The mass flow rate of state 39 is also calculated from the following equation:

$$m_{46} = m_{43} - m_{45} \quad (13)$$

The concentration of salt in the effluent from the desalination plant is presented as fresh water at state 38 and the rejected water at state 39 as the following equations:

$$X_d = X_f(1 - SR) \quad (14)$$

$$X_b = \frac{m_{43}X_f - m_{45}X_d}{m_{46}} \quad (15)$$

The average salt concentration is also presented below:

$$X_{av} = \frac{m_{43}X_f - m_{45}X_b}{m_{45}} \quad (16)$$

The following is the temperature correction relation as follows:

$$TCF = exp\left(2700\left(\frac{1}{T_k} - \frac{1}{298}\right)\right) \quad (17)$$

The relationship of water permeability in the membrane is introduced below:

$$k_w = \frac{6.84e-8 \times (18.6865 - (0.177 \times X_d))}{T_k} \quad (18)$$

Here is three relationships for mean osmotic pressure, maximum osmotic pressure in the membrane, and membrane pressure difference:

$$P_{av} = 37.92(X_f + X_b) \quad (19)$$

$$P_{net} = P_{av} - 75.84X_d \quad (20)$$

$$\Delta P = \frac{m_{45}}{3600 \times TCF \times FF \times A_e \times n_e \times n_v \times k_w} + P_{net} \quad (21)$$

Finally, the working relationship required for the high-pressure pump is introduced as follows:

$$\Delta P = \frac{1000 \times m_{43} \times \Delta P}{3600 \times \rho_f \times \eta_p} \quad (22)$$

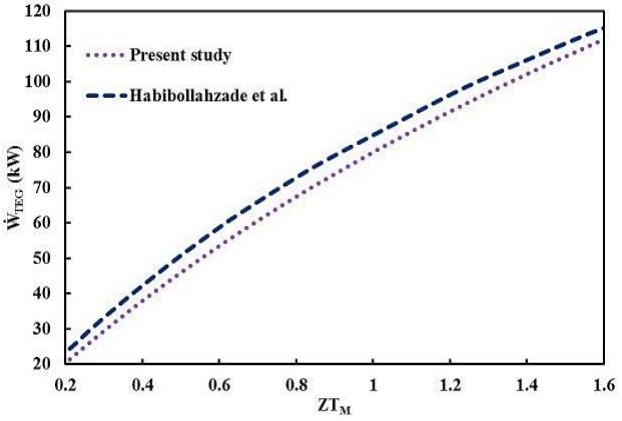

Fig. 2: Validation of the present work with the work of Habibollahzadeh et al. [20]

Validation

Thermoelectrics can be divided into two general categories: heating-cooling thermoelectrics and generator thermoelectrics. In heating-cooling thermoelectrics, the difference in electrical potential between the two ends of a semiconductor wire will cause a temperature difference between the two ends [18], which may be used for heating or cooling purposes. On the other hand, in thermoelectric generators based on the tuber effect, the temperature difference between the two ends of the semiconductor causes a potential difference in it [19-25].

To validate the results and the work done, the thermoelectric subsystem will be validated for the validation of the present study. Therefore, the present work was compared with *Mr. Habibollahzadeh et al*. [20]. In Figure 2, the desired results are evaluated.

RESULTS AND DISCUSSION

The amount of sunlight is one of the factors that has a very significant effect on system performance. Figures 3 (a) and (b) show the effect of solar radiation on running costs, output work, cooling load, freshwater production, and exergy efficiency.

In general, the amount of sunlight increases efficiency and increases the amount of output work. Of course, due to the existence of wind turbines and their greater impact on the system, the existence of irreversibility in the solar system with a parabolic-linear collector occurs and reduces the total exergy of the output. The total efficiency of exergy decreases from 36.97 to 25.59%, which shows a decrease of 10%. As the solar radiation increases, the inlet fluid to the solar system and steam turbine increases. As a

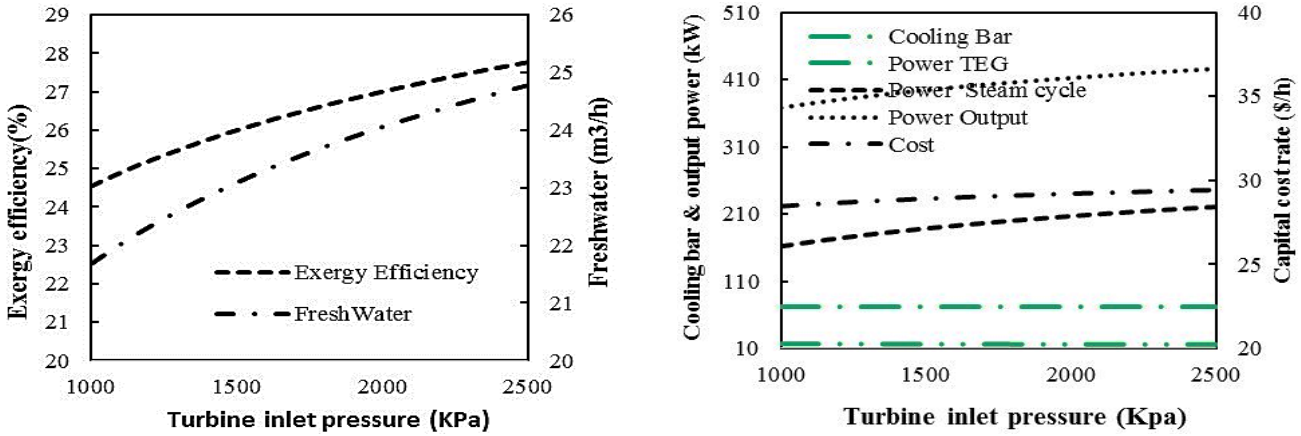

Fig. 3: Impact of solar radiation on running costs, output work and cooling load, freshwater production, and total output exergy.

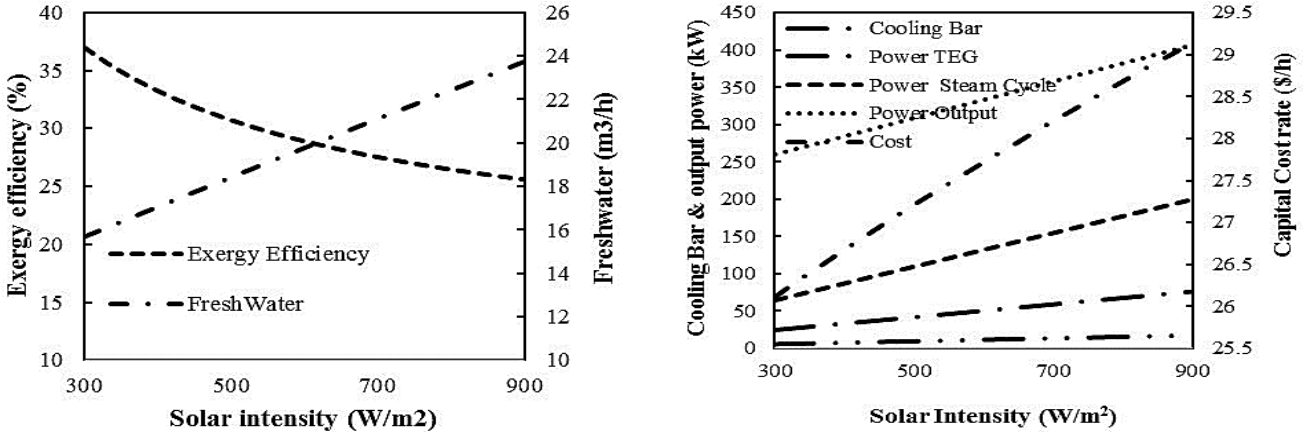

Fig. 4: Effect of turbine inlet pressure on running costs, output work and cooling load, freshwater production, and total output exergy.

result, as the flow rate increases, the output of the steam cycle also increases, which will increase the total output work. The total output is about 147 kW and increases by 56%. As the total output increases, the cost of supplying equipment also increases. Figure 3a shows that system costs increased with increasing solar radiation intensity; as the electricity produced in the system increases, the flow of freshwater production increases. Due to the increased flow rate, the cooling load increases in the single-effect absorption refrigeration cycle [26-35].

Figure 4 shows the effect of inlet pressure on the turbine on running costs, outlet work and cooling load, freshwater production, and exergy of the total output. The enthalpy of the fluid entering the turbine increases, and as a result, the work of the turbine, the steam cycle, and the total work of the output increases. The total output increased from 368.5 to 423.3, which is about 14%.

As the system's output increased, so did the cost of the system, the freshwater produced, and the output's total output. System costs increased from 28.5 to 29.5, which is not a significant amount [36-45].

Another important parameter of the system is the exhaust pressure system of the steam turbine, which in Figure 5 (a) and (b) its effect on current costs, output work and cooling load, freshwater production, and total exergy were examined. The output pressure from the turbine reduced the amount of work generated by the steam cycle. It reduced the exergy efficiency, but as the output pressure increased, the enthalpy of the input fluid to the thermoelectric increased, increasing the work produced by the thermoelectric. It is very significant since the reduction of turbine output work has a much greater impact on the total output work and the exergy of the system. As a result, the total output work and the total exergy are reduced. 29.2 to 28.4 The amount of freshwater produced decreases from 23.9 to 21.3. Also, with increasing turbine outlet pressure and enthalpy, more heat is transferred to the absorption refrigeration cycle generator and the cooling load increases from 69.4 to 78.4.

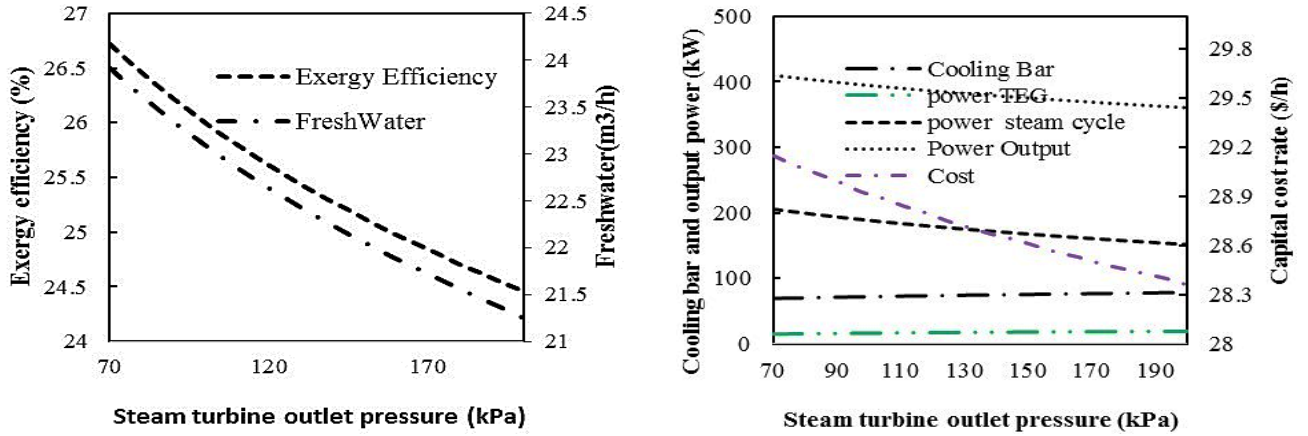

Fig. 5: Effect of turbine outlet pressure on running costs, outlet work and cooling load, freshwater production, and total outlet exergy

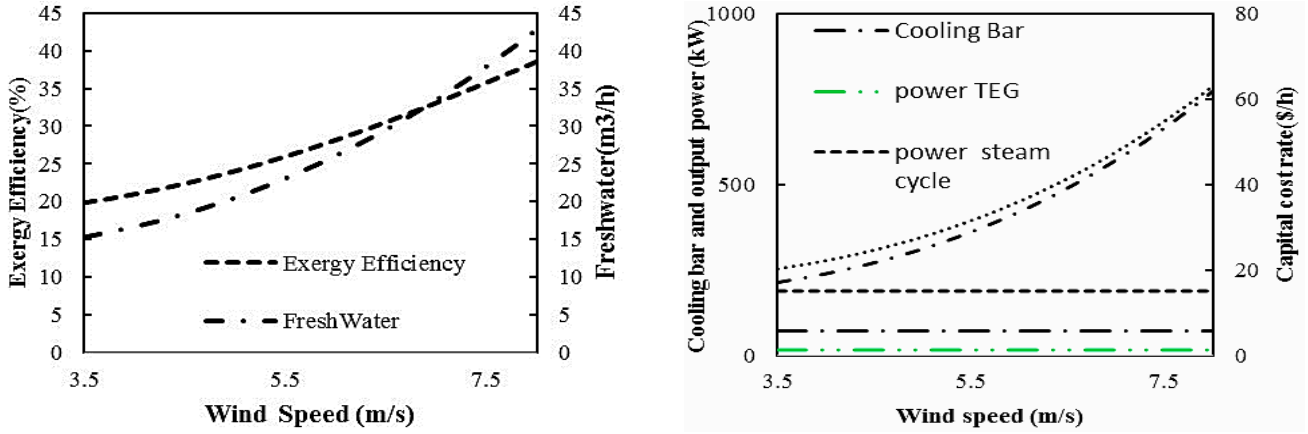

Fig. 6: Effect of average wind speed on running costs, output work and cooling load, freshwater production, and total output exergy.

Figure 6 (a) and (b) show the effect of average wind speed on running costs, output work and cooling load, freshwater production, and exergy of the total output. As the wind speed increases, the output of the wind turbine increases and increases. The total output work and exergy will be the whole system, resulting from which the amount of freshwater produced and the system costs will increase. The total output work at an average speed of 3.5 m/s equals 254 kW and at a speed of 8 m/s equals 789 kW [46, 47].

Figure 7 investigates the effect of ambient temperature parameters on the number of exergy losses of system components. As shown in Figure 7, the exergy losses of the solar system are higher than the other components and increase with increasing solar radiation from 398 to 1179. Exergy losses have increased by about 196% with increasing solar radiation. Also, with the increase of solar radiation, the exergy losses of the steam cycle components, including the evaporator, steam, thermoelectric turbine, and pump 2, increase the amount of steam cycle exergy losses. The results showed increased exergy losses for the absorption refrigeration cycle and reversed osmosis desalination water.

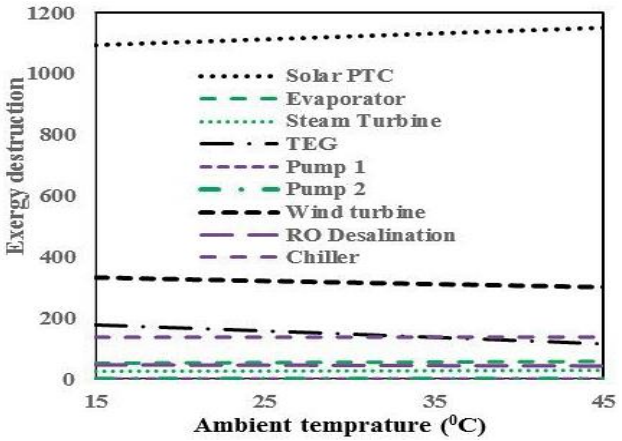

Fig. 7: Investigation of the effect of the ambient temperature of exergy losses on system components' rate of exergy losses.

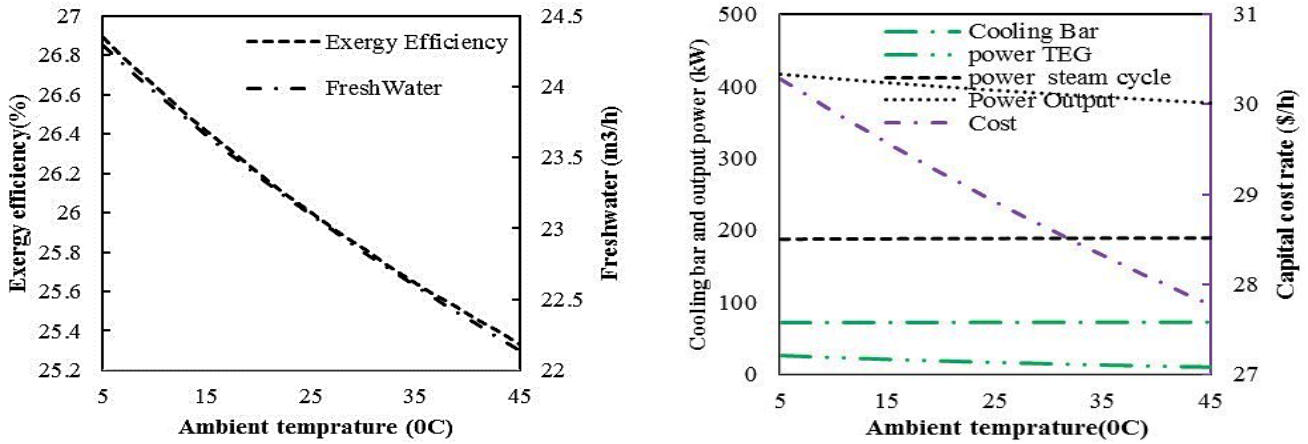

Fig. 8: The effect of ambient temperature on cost, output work and cooling load, freshwater production, and total output exergy.

Figure 7 investigates the effect of an important parameter of ambient temperature on the number of exergy losses of system components. As shown in Figure 7, with increasing ambient temperature, the exergy losses of the solar system, evaporator, steam turbine, pumps 1 and 2, and single-effect absorption refrigeration cycle increase, with the highest percentage increase for the evaporator at 11%. The amount of evaporator exergy losses have increased from 52 to 58 due to ambient temperature on the evaporator. Also, wind turbine exergy losses, reverse osmosis, and thermoelectric desalination water has decreased with increasing ambient temperature. The highest reduction percentage is obtained for thermoelectric, and 54% is obtained. The number of thermoelectric exergy losses has decreased from 17.5 to 115.5 due to ambient temperature on the thermoelectric for the 9 and 10 points shown in the designed schematic of the cycle.

Figures 8 (a) and (b) show the effect of ambient temperature on running costs, output work and cooling load, freshwater production, and exergy of total output. As the ambient temperature increases, the air density decreases with decreasing air density and the output work rate decreases. The wind turbine has reduced the total output from 417 to 377 kW. With the output decrease, the total output of fresh water and total exergy has also decreased.

Steam cycle and absorption refrigeration cycle the work of the steam cycle and the cooling load of the refrigeration cycle increase, but the decrease in wind turbine output has a greater effect on the total output work and ultimately decreases it. However, the increased ambient temperature on the thermoelectric generator at 9 points and 10 designed schematics reduced the thermoelectric work from 26 to 9.8. This reduction in the thermoelectric work also affected the reduction of the total output work.

In Table 2, the sensitivity analysis of the effect of the studied parameters on the outputs of the studied system is based on solar, and wind energy, and the percentage of growth or decrease of the graphs was calculated.

Table 2 concludes that wind speed has the most change on total work and cost rate, which has led to a high increase in efficiency and system work, which is introduced as the most effective parameter in these studies, but according to the results of wind speed changes on thermoelectric work no Has affected. After wind speed, the most impact on system outputs is the intensity of solar radiation and inlet pressure to the turbine. Ambient temperature also reduces the efficiency of exergy and freshwater produced by the system.

CONCLUSIONS

In the present study, the solar system with parabolic-linear collector and wind energy has been used as a source of energy supply. The multiple energy production systems are designed to meet existing needs. Finally, the results showed that solar radiation, wind energy, output, and freshwater production suit the multiple production systems introduced for the required applications. Other main research results are as: with increasing solar radiation, the amount of freshwater produced for the system increased from 15.69 to 23.75 kg/h; and with increasing the inlet pressure to the steam turbine, the total exergy efficiency for the system increased from 24.54 to 27.77%. As the ambient temperature increased, the total costs for the system decreased from 30.28 to 27.77 $/s. Also according to the results, solar energy with the central receiver has the

Table 2: Sensitivity analysis.

Parameter	Freshwater (kg/h)	Cost rate ($/h)	Exergy efficiency (%)	Thermoelectric power (kW)	Total power (kW)
Solar radiation	Max: 23.75 Min: 15.69 Var%: 51.37	Max: 29.14 Min: 26.11 Var%:11.6	Max: 36.97 Min: 25.59 Var%: 44.64	Max: 17.35 Min: 5.604 Var%: 209.60	Max: 406.8 Min: 260 Var%: 56.46
Wind speed	Max: 42.82 Min: 15.33 Var%: 179.32	Max: 61.9 Min: 17.13 Var%: 261.35	Max: 38.56 Min: 19.88 Var%: 93.96	Max: 16.37 Min: 16.37 Var%: 0	Max: 789.1 Min: 253.6 Var%: 211.15
Environment temperature	Max: 24.29 Min: 22.14 Var%: 9.71	Max: 30.28 Min: 27.77 Var%: 9.03	Max: 26.89 Min: 25.33 Var%: 6.15	Max: 25.96 Min: 9.834 Var%: 163.98	Max: 417 Min: 377 Var%: 10.61
Inlet pressure to the turbine	Max: 24.78 Min: 21.68 Var%: 14.29	Max: 29.44 Min: 28.47 Var%: 3.40	Max: 27.77 Min: 24.54 Var%: 13.16	Max: 16.82 Min: 15.82 Var%: 6.32	Max: 426.3 Min: 368.5 Var%: 15.68
Output pressure from the turbine	Max: 23.92 Min: 21.25 Var%:12.56	Max: 29.15 Min: 28.36 Var%: 2.78	Max: 26.72 Min: 24.46 Var%: 9.23	Max: 19.23 Min: 14.86 Var%: 29.40	Max: 410.1 Min: 360.5 Var%: 13.75

highest exergy losses. The exergy losses showed that the solar system with 60% and wind turbines with 17% have the highest exergy losses in the system components.

Received: May. 28, 2022 ; Accepted: Aug. 22, 2022

References

[1] Gupta D.K., Kumar R., Kumar N., Performance Analysis of PTC field based Ejector Organic Rankine Cycle Integrated with a Triple Pressure Level Vapor Absorption System (EORTPAS), *Engineering Science and Technology, an International Journal*, **23(1):** 82-91 (2020).

[2] Kerme E.D., Orfi J., Fung A.S., Salilih, E.M., Khan S.U.D., Alshehri H., Alrasheed M., Energetic and Exergetic Performance Analysis of a Solar Driven Power, Desalination and Cooling Poly-Generation System, *Energy*, **196:** 117150 (2020).

[3] Alirahmi S.M., Dabbagh S.R., Ahmadi P., Wongwises S., Multi-Objective Design Optimization of a Multi-Generation Energy System based on Geothermal and Solar Energy, *Energy Conversion and Management*, **205:** 112426 (2020).

[4] Alotaibi S., Alotaibi F., Ibrahim O.M., Solar-Assisted Steam Power Plant Retrofitted with Regenerative System using Parabolic Trough Solar Collectors, *Energy Reports*, **6:** 124-133 (2020).

[5] Ehyaei M.A., Ahmadi A., Assad M.E.H., Salameh T., Optimization of Parabolic through Collector (PTC) with Multi Objective Swarm Optimization (MOPSO) and Energy, Exergy and Economic Analyses, *Journal of Cleaner Production*, **234:** 285-296 (2019).

[6] Toghyani S., Afshari E., Baniasadi E., Shadloo M.S., Energy and Exergy Analyses of a Nanofluid based Solar Cooling and Hydrogen Production Combined System, *Renewable Energy*, **141:** 1013-1025 (2019).

[7] AlZahrani A.A., Dincer I., Energy and Exergy Analyses of a Parabolic trough Solar Power Plant using Carbon Dioxide Power Cycle, *Energy Conversion and Management*, **158:** 476-488 (2018).

[8] Yilmaz F., Energy, Exergy and Economic Analyses of a Novel Hybrid Ocean Thermal Energy Conversion System for Clean Power Production, *Energy Conversion and Management*, **196:** 557-566 (2019).

[9] Ishaq H., Dincer I., Evaluation of a Wind Energy-Based System for Co-Generation of Hydrogen and Methanol Production, *International Journal of Hydrogen Energy*, **45(32):** 15869-15877 (2020).

[10] Bamisile O., Huang Q., Li J., Dagbasi M., Kemena A.D., Abid M., Hu W., Modelling and Performance Analysis of an Innovative CPVT, Wind and Biogas Integrated Comprehensive Energy System: An Energy and Exergy Approach, *Energy Conversion and Management*, **209:** 112611 (2020).

[11] Kianfard H., Khalilarya S., Jafarmadar S., Exergy and Exergoeconomic Evaluation of Hydrogen and Distilled Water Production via Combination of PEM Electrolyzer, RO Desalination Unit and Geothermal Driven Dual Fluid ORC, *Energy Conversion and Management*, **177:** 339-349 (2018).

[12] Alirahmi S.M., Assareh E., Energy, Exergy, and Exergoeconomics (3E) Analysis and Multi-Objective Optimization of a Multi-Generation Energy System for Day and Night Time Power Generation-Case Study: Dezful City, *International Journal of Hydrogen Energy*, **45(56):** 31555-31573 (2020).

[13] Mohammadi K., Khaledi M.S.E., Saghafifar M., Powell K., Hybrid Systems based on Gas Turbine Combined Cycle for Trigeneration of Power, Cooling, and Freshwater: A Comparative Techno-Economic Assessment, *Sustainable Energy Technologies and Assessments*, **37:** 100632 (2020).

[14] Haghanimanesh M., Baniasadi E., Kerdabadi J.K., Yu X., Exergoeconomic Analysis of a Novel Trigeneration Cycle based on Steel Slag Heat Recovery and Biogas Production in Steelmaking Plants, *Ene. Con. Manag.*, **263:** 115688 (2022).

[15] Fakhari I., Peikani P., Moradi M., Ahmadi P., An Investigation of Optimal Values in Single and Multi-Criteria Optimizations of a Solar Boosted Innovative Tri-Generation Energy System, *Journal of Cleaner Production*, **316:** 128317 (2021).

[16] Musharavati F., Khanmohammadi S., Pakseresht A., Proposed A New Geothermal based Poly-Generation Energy System Including Kalina Cycle, Reverse Osmosis Desalination, Elecrolyzer Amplified with Thermoelectric: 3E Analysis and Optimization, *Applied Thermal Engineering*, **187:** 116596 (2021).

[17] Cao Y., Delpisheh M., Yousefiasl S., Athari H., El-Shorbagy M.A., Jarad F., Wae-hayee M., Examination and Optimization of a Novel Auxiliary Trigeneration System for a Ship through Waste-to-Energy from its Engine, *Case Studies in Thermal Engineering*, **31:** 101860 (2022).

[18] Zhou Z., Cao Y., Anqi A.E., Zoghi M., Habibi H., Rajhi A.A., Alamri S., Converting a Geothermal-Driven Steam Flash Cycle into a High-Performance Polygeneration System by Waste Heat Recovery: 3E Analysis and Genetic-Fgoalattain Optimization, *Renewable Energy*, **186:** 609-627 (2022).

[19] Razmi A.R., Janbaz, M., Exergoeconomic Assessment with Reliability Consideration of a Green Cogeneration System based on Compressed Air Energy Storage (CAES), *Ene. Conv. Manag.*, **204:** 112320 (2020).

[20] Rashidi H., Khorshidi J., Exergoeconomic Analysis and Optimization of a Solar based Multigeneration System using Multiobjective Differential Evolution Algorithm, *J. Clea. Prod.*, **170:** 978-990 (2018).

[21] Nemati A., Sadeghi M., Yari M., Exergoeconomic Analysis and Multi-Objective Optimization of a Marine Engine Waste Heat Driven RO Desalination System Integrated with an Organic Rankine Cycle using Zeotropic Working Fluid, *Desalination*, **422:** 113-123 (2017).

[22] Naseri A., Bidi M., Ahmadi M.H., Saidur R., Exergy Analysis of a Hydrogen and Water Production Process by a Solar-Driven Transcritical CO_2 Power Cycle with Stirling Engine, *J. Clear Prod.*, **158:** 165-181 (2017).

[23] Talebi S., Norouzi N., Entropy and Exergy Analysis and Optimization of the VVER Nuclear Power Plant with a Capacity of 1000 MW using the Firefly Optimization Algorithm, *Nuclear Engineering and Technology*, **52(12):** 2928-2938 (2020).

[24] Norouzi N., 4E Analysis of a Fuel Cell and Gas Turbine Hybrid Energy System, *Biointerface Res. Appl. Chem.*, **11:** 7568-7579.

[25] Norouzi N., Talebi S., Exergy and Energy Analysis of Effective Utilization of Carbon Dioxide in the Gas-to-Methanol Process, *Iran. J. Hy. F. C.*, **7(1):** 13-31 (2020).

[26] Norouzi N., 4E Analysis and Design of a Combined Cycle with a Geothermal Condensing System in Iranian Moghan Diesel Power Plant, *International Journal of Air-Conditioning and Refrigeration*, **28(3):** 2050022 (2020).

[27] Algieri A., Morrone P., Energetic Analysis of Biomass-Fired ORC Systems for Micro-Scale Combined Heat and Power (CHP) Generation. A Possible Application to the Italian Residential Sector, *Applied Thermal Engineering*, **71(2):** 751-759 (2014).

[28] Norouzi N., Hosseinpour M., Talebi S., Fani M., A 4E Analysis of Renewable Formic Acid Synthesis from the Electrochemical Reduction of Carbon Dioxide and Water: Studying Impacts of the Anolyte Material on the Performance of the Process, *Journal of Cleaner Production*, **293:** 126149 (2021).

[29] Mahmoud M., Ramadan M., Naher S., Pullen K., Abdelkareem M.A., Olabi A.G. A Review of Geothermal Energy-Driven Hydrogen Production Systems, *Thermal Science and Engineering Progress*, **22:** 100854 (2021).

[30] Parham K, Assadi M., A Parametric Performance Analysis of a Novel Geothermal based Cogeneration System, "Sustainable Energy Technology and Policies: A Transformational Journey", Springer, Singapore 167-182 (2018).

[31] Han J., Wang X., Xu J., Yi N., Talesh S.S., Thermodynamic Analysis and Optimization of an Innovative Geothermal-based Organic Rankine Cycle using Zeotropic Mixtures for Power and Hydrogen Production, *International Journal of Hydrogen Energy*, **45(15):** 8282-99 (2020).

[32] Yuksel Y.E., Ozturk M., Dincer I., Energetic and Exergetic Performance Evaluations of a Geothermal Power Plant based Integrated System for Hydrogen Production, *International Journal of Hydrogen Energy*, **43(1):** 78-90 (2018).

[33] Cao Y., Dhahad H.A., Togun H., Hussen H.M., Rashid T.A., Anqi A.E., Farouk N., Issakhov A., Exergetic and Financial Parametric Analyses and Multi-Objective Optimization of a Novel Geothermal-Driven Cogeneration Plant; Adopting a Modified Dual Binary Technique, *Sustainable Energy Technologies and Assessments*, **48:** 101442 (2021).

[34] Cao L., Lou J., Wang J., Dai Y., Exergy Analysis and Optimization of a Combined Cooling and Power System Driven by Geothermal Energy for Ice-Making and Hydrogen Production, *Energy Conversion and Management*, **174:** 886-896 (2018).

[35] Yilmaz C., Koyuncu I., Alcin M., Tuna M., Artificial Neural Networks based Thermodynamic and Economic Analysis of a Hydrogen Production System Assisted by Geothermal Energy on Field Programmable Gate Array, *International Journal of Hydrogen Energy*, **44(33):** 17443-17459 (2019).

[36] Raei B., Ghadi A., Bozorgian A., "Heat Integration of Heat Exchangers Network Using Pinch Technology", *19th International Congress of Chemical and Process Engineering CHISA*, (2010).

[37] Pourabadeh A., Nasrollahzadeh B., Razavi R., Bozorgian A., Najafi M., A.Oxidation of FO and N_2 Molecules on the Surfaces of Metal-Adopted Boron Nitride Nanostructures as Efficient Catalysts, *J. Struct. Chem.*, **59:** 1484-1491 (2018).

[38] Esmaeili Bidhendi M., Asadi Z., Bozorgian A., et al., New Magnetic Co_3O_4/Fe_3O_4 doped Polyaniline Nanocomposite for the Effective and Rapid Removal of Nitrate Ions from Ground Water Samples, *Environ. Prog. Sustainable Energy.*, **39:** e13306 (2019).

[39] Bozorgian A., Arab Aboosadi Z., Mohammadi A., Honarvar B., Azimi A., Optimization of Determination of CO_2 Gas Hydrates Surface Tension in the Presence of non-Ionic Surfactants and TBAC, *Eurasian Chem. Commun.*, **2:** 420-426 (2020).

[40] Mashhadizadeh J., Bozorgian A., Azimi A., Investigation of the Kinetics of Formation of Clatrit-Like Dual Hydrates TBAC in the Presence of CTAB, *Eurasian Chem. Commun.*, **2:** 536-547 (2020).

[41] Norouzi N., Bozorgian A., Dehghani M., Best Option of Investment in Renewable Energy: A Multicriteria Decision-Making Analysis for Iranian Energy Industry, *Journal of Environmental Assessment Policy and Management*, **22(01n02):** 2250001 (2020).

[42] Norouzi N., Ebadi A., Bozorgian A., Hoseyni S.J., Vessally E., Energy and Exergy Analysis of Internal Combustion Engine Performance of Spark Ignition for Gasoline, Methane, and Hydrogen Fuels, *Iran. J. Chem. Chem. Eng. (IJCCE)*, **40(6):** 1909-1930 (2021).

[43] Bozorgian A., Arab Aboosadi Z., Mohammadi A., Honarvar B., Azimi A., Statistical Analysis of the Effects of Aluminum Oxide (Al_2O_3) Nanoparticle, TBAC, and APG on Storage Capacity of CO_2 Hydrate Formation, *Iran. J. Chem. Chem. Eng. (IJCCE)*, **41(1):** 220-231 (2022).

[44] Ahmadpour A., Bozorgian A., Eslamimanesh A., Mohammadi A.H., Photocatalytic Treatment of Spontaneous Effluent of Petrochemical Effluents by TiO_2 CTAB Synthetic Nanoparticles, *Desalin. Water Treat.*, **249:** 297-308 (2022).

[45] Norouzi N., Ebadi A., Bozorgian A., Hoseyni S.J., Vessally E., Cogeneration System of Power, Cooling, and Hydrogen from Geothermal Energy: An Exergy Approach, *Iran. J. Chem. Chem. Eng. (IJCCE)*, **41(2):** 706-721 (2022).

[46] Bozorgian A., Arab Aboosadi Z., Mohammadi A., Honarvar B., Azimi A., Determination of CO_2 gas Hydrates Surface Tension in the Presence of Nonionic Surfactants and TBAC, *Rev. Roum. Chim.*, **65:** 1061-1065 (2020).

[47] Kanani M., Kanani N., Batooie N., Bozorgian A., Barghi A., Rezania S., Removal of Rhodamine 6G Dye using One-Pot Synthesis of Magnetic Manganese Graphene Oxide: Optimization by Response Surface Methodology, *Environ. Nanotechnol., Monit. Manage.*, **18:** 100709 (2022).